A Large Air Gap 3 kW Wireless Power Transfer System for Electric Vehicles

Hiroya Takanashi*, Yukiya Sato*, Yasuyoshi Kaneko*, Shigeru Abe*, Tomio Yasuda**
*Saitama University, Saitama, Japan
** Technova Inc., Tokyo, Japan
s11mm222@mail.saitama-u.ac.jp

***Abstract*— A wireless power transfer system for electric vehicles is required to have high efficiency, a large air gap, and good tolerance for misalignment in the lateral direction and to be compact and lightweight. A new 3 kW transformer has been developed to satisfy these criteria using a novel H-shaped core and split primary capacitors. The design procedure based on the coupling factor *k*, the winding's *Q*, and the core loss is described. An efficiency of 90% was achieved across a 200 mm air gap.**

I. INTRODUCTION

The development and commercialization of plug-in hybrid electric vehicles (PHVs) and electric vehicles (EVs) are actively being realized due to environmental concerns and rising oil prices. PHVs and EVs currently need to be connected to power supplies by electrical wires to charge their batteries. A wireless power transfer system for electric vehicles (such as that depicted in Fig. 1) would have many advantages, such as having the convenience of being wireless and enabling high-power charging to be performed safely [1, 2]. Therefore, wireless power transfer systems are being studied around the world. Wireless power transfer systems for electric vehicles must have high efficiency, a large air gap, and good tolerance for misalignment in the lateral direction and be compact and lightweight [3].

There are two types of methods used in wireless power transfer systems: inductive coupling methods [1, 2, 3] and magnetic resonance methods [4, 5]. The inductive coupling methods use a frequency lower than 200 kHz, use ferrite cores, and have coupling factors above 0.1. On the other hand, the magnetic resonance methods use a frequency higher than 1 MHz, do not use ferrite cores, and have coupling factors below 0.1.

Recently, research on the inductive coupling methods used for PHVs and EVs has adopted rectangular cores instead of the conventional circular cores. For example, these include Flux pipes [1], Double-D-Quadrature (DDQ) structures [2], and H-shaped cores [3].

To compensate for leakage inductance, the inductive coupling methods usually adopt the series and parallel capacitor methods (SP methods) [3] or parallel and parallel capacitor methods (PP methods) [1, 2]. It is known that the magnetic resonance methods can be represented by an equivalent circuit of the series and series capacitor methods (SS methods) [5].

Inductive coupling methods and magnetic resonance methods have not been compared in terms of their efficiency because they use different frequencies and differ in their use of ferrite cores. In this paper, we compare the efficiencies of the two methods using the coupling factor *k* and the winding's *Q* values when considering the copper loss only.

The results show that the maximum efficiencies of the SP methods and SS methods are given by the same simple equations of *k* and *Q*, and those equations indicate that *k* and *Q* must be increased in order to increase the efficiency.

A large air gap 3 kW transformer of the inductive coupling type is developed using this efficiency equation. To increase the coupling factor *k*, we adopt an H-shaped core and a wide winding width. To increase the winding's *Q*, we increase the input frequency.

The experimental results show that this large air gap 3 kW transformer has an efficiency of over 90% for a gap length of 200 mm. The results for the gap changes (160 mm ± 40 mm) and misalignments (forward ± 100 mm, lateral ±

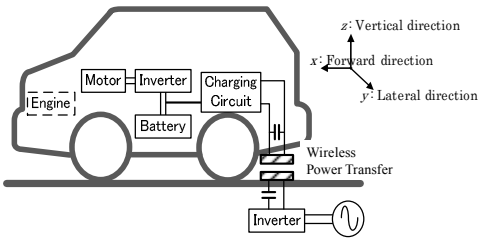

Figure 1. Wireless power transfer system of an EV.

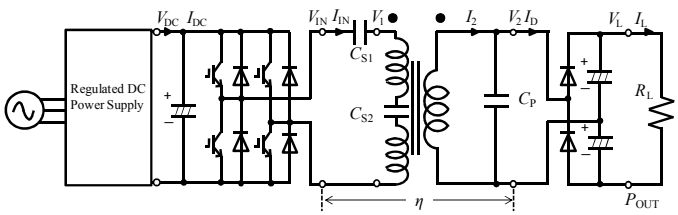

Figure 2. Wireless power transfer system configuration.

200 mm) are also presented. Adopting the H-shaped core, the transformer is small in size (320 × 300 × 40 mm) and lightweight (5.5 kg).

The purpose of this paper is to introduce the maximum efficiencies of the inductive coupling methods and magnetic resonance methods using the same simple equations when considering the copper loss only, to propose the design procedure for the inductive coupling type using this equation, and to present a newly designed 3 kW transformer. This transformer has high efficiency, a large air gap, and good tolerance for misalignments in the lateral direction and is compact and lightweight.

II. Maximum Efficiency of Wireless Power Transfer System Using k and Q

A. Series and Parallel Resonant Capacitor Methods (Inductive Coupling Method)

Fig. 2 shows a schematic diagram of the wireless power transfer system with series and parallel resonant capacitor (SP methods). A full-bridge inverter is used as a high-frequency power supply. A double-voltage rectifier is used as a rectifier circuit on the second side to raise the efficiency. The cores are made of ferrite, and litz wires are used for the windings.

1) Equivalent Circuit

Fig. 3 (a) shows a detailed equivalent circuit. It consists of a T-shaped equivalent circuit to which the primary series capacitor C_S, secondary parallel capacitor C_P, and load resistance R_L have been added. The primary values are converted into secondary equivalent values using the turn ratio $a = N_1/N_2$. Since the winding resistances r'_1 and r_2 and the ferrite core loss r'_0 are considerably lower than the leakage reactance x'_1 and x_2 and the mutual reactance x'_0 at the resonant frequency, the winding resistances. The ferrite core loss is ignored. Here, M is the mutual inductance ($x'_0 = \omega_0 M/a$). The rectifier is also omitted, and a secondary circuit for analysis consists of C_P and the load resistance R_L.

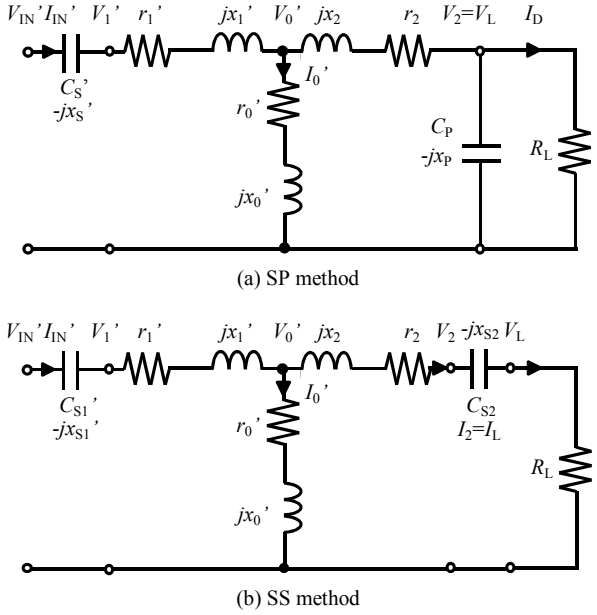

Figure 3. Detailed equivalent circuit of wireless power transfer systems.

2) Characteristics of Series and Parallel Resonant Capacitor Methods

To achieve resonance of the input frequency f_0 ($=\omega_0/2\pi$) with the self-inductance of the secondary winding L_2, which is equivalent to adding a mutual reactance x'_0 and a leakage reactance x_2, the secondary parallel capacitor C_P is given by:

$$\frac{1}{\omega_0 C_P} = \omega_0 L_2 = x_P = x'_0 + x_2 \tag{1}$$

The primary series capacitor C_S (C'_S denotes its secondary equivalent) is determined as:

$$\frac{1}{\omega_0 C'_S} = x'_S = x'_1 + \frac{x'_0 x_2}{x'_0 + x_2} \tag{2}$$

V'_{IN} and I'_{IN} can be expressed as:

$$V'_{IN} = V_{IN}/a = bV_2, \quad I'_{IN} = I_D/b, \quad b = \frac{x'_0}{x'_0 + x_2} \tag{3}$$

These equations suggest that the equivalent circuit of a transformer with these capacitors is the same as an ideal transformer at the resonant frequency.

Ignoring the ferrite core loss ($r_0 = 0$), the efficiency can be approximated by:

$$\eta = \frac{R_L I_L^2}{R_L I_L^2 + r'_1 I'^2_{IN} + r'_2 I'^2_2} = \frac{R_L}{R_L + \frac{r'_1}{b^2} + r_2\left\{1 + \left(\frac{R_L}{x_P}\right)^2\right\}} \tag{4}$$

The maximum efficiency $\eta_{max\ SP}$ is obtained when $R_L = R_{Lmax\ SP}$.

$$R_{Lmax\,SP} = x_P\sqrt{\frac{1}{b^2}\frac{r'_1}{r_2} + 1}\,, \eta_{max\,SP} = \frac{1}{1 + \frac{2r_2}{x_P}\sqrt{\frac{1}{b^2}\frac{r'_1}{r_2} + 1}} \tag{5}$$

If these characteristics are used, it is possible to design a transformer that has a maximum efficiency when the output power is equal to the rated power.

3) Maximum Efficiency of Series and Parallel Resonant Capacitor Methods using k and Q

The coupling factor k, the primary winding's Q_1, and the secondary winding's Q_2 are represented by:

$$k = \frac{M}{\sqrt{L_1 L_2}}, \quad Q_1 = \frac{\omega L_1}{r_1}, \quad Q_2 = \frac{\omega L_2}{r_2} \tag{6}$$

Here, L_1 is the self-inductance of the primary winding ($L_1 = a^2(x'_1 + x'_0)/\omega_0$).

If k is lower than 0.3 and $Q_1 \cong Q_2$,

$$\frac{1}{k^2}\frac{Q_2}{Q_1} >> 1 \tag{7}$$

Then, these equations can be expressed using k and Q.

TABLE I. $\eta_{\max}$ AND $R_{\mathrm{L}\max}$ FOR EACH METHOD.

Resonant capacitor	$\eta_{\max}$	$R_{\mathrm{L}\max}$
SP	$\dfrac{1}{1+\dfrac{2}{k\sqrt{Q_1Q_2}}}$	$\dfrac{r_2Q_2}{k}\sqrt{\dfrac{Q_2}{Q_1}}$
PP		$\dfrac{r_2Q_2}{k}\sqrt{\dfrac{Q_2}{Q_1}}$
SS		$kr_2\sqrt{Q_1Q_2}$

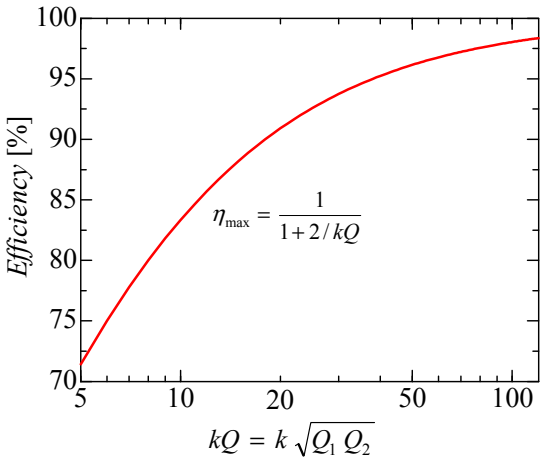

Figure 4. Relationship between $\eta_{\max}$ and kQ.

$$R_{\mathrm{Lmax\ SP}}=\frac{r_2Q_2}{k}\sqrt{\frac{Q_2}{Q_1}},\ \eta_{\max\mathrm{SP}}=\frac{1}{1+\dfrac{2}{k\sqrt{Q_1Q_2}}} \tag{8}$$

By following the same steps, the $R_{\mathrm{Lmax\ PP}}$ and $\eta_{\max\mathrm{PP}}$ of the PP methods can be derived. Table I lists the equations for the maximum efficiency $\eta_{\max}$ and R_{Lmax} of the SP methods, PP methods, and SS methods. From Table I, the equation for the maximum efficiency of the PP methods is the same as that of the SP methods [6].

B. *Series and Series Resonant Capacitor Methods (Magnetic Resonance Methods)*

1) *Equivalent Circuit*

The magnetic resonance methods can be represented by an equivalent circuit of the series capacitors methods. Fig. 3 (b) shows a typical detailed equivalent circuit with series capacitors (SS methods). It consists of a T-shaped equivalent circuit to which the primary series capacitor C_{S1}, the secondary series capacitor C_{S2}, and the load resistance R_{L} have been added.

2) *Characteristics of Series and Series Resonant Capacitor Methods*

To achieve resonance with the self-inductance of the primary winding L_1 and the secondary winding L_2, the primary series capacitor C_{S1} and the secondary series capacitor C_{S2} are given by:

$$\frac{1}{\omega_0 C'_{\mathrm{S1}}}=x'_{\mathrm{S1}}=x'_0+x'_1\quad \frac{1}{\omega_0 C_{\mathrm{S2}}}=x_{\mathrm{S2}}=x'_0+x_2 \tag{9}$$

and V'_{IN} and I'_{IN} can be expressed as:

$$V'_{\mathrm{IN}}=-jx'_0 I_{\mathrm{L}}\quad I'_{\mathrm{IN}}=-j\frac{1}{x'_0}V_{\mathrm{L}} \tag{10}$$

These equations suggest that the equivalent circuit for a transformer with these capacitors has the same characteristics as the immittance converter at the resonant frequency.

3) *Maximum Efficiency of Series and Series Resonant Capacitor Methods using k and Q*

The equation for the maximum efficiency of the SS methods is given by:

$$R_{\mathrm{Lmax\ SS}}=x'_0\sqrt{\frac{r_2}{r'_1}},\ \eta_{\max\mathrm{SS}}=\frac{1}{1+\dfrac{2r_2}{x'_0}\sqrt{\dfrac{r'_1}{r_2}}} \tag{11}$$

Then, these equations can be expressed using k and Q.

$$R_{\mathrm{Lmax\ SS}}=kr_2\sqrt{Q_1Q_2},\ \eta_{\max\mathrm{SS}}=\frac{1}{1+\dfrac{2}{k\sqrt{Q_1Q_2}}} \tag{12}$$

The $\eta_{\max\mathrm{SS}}$ in (12) is equal to the $\eta_{\max\mathrm{SP}}$ in (8).

Fig. 4 shows the relationship between the maximum efficiency $\eta_{\max}$ and kQ $(=k\sqrt{Q_1Q_2}$)of (8) and (12). Larger values of k and Q realize a higher maximum efficiency $\eta_{\max}$.

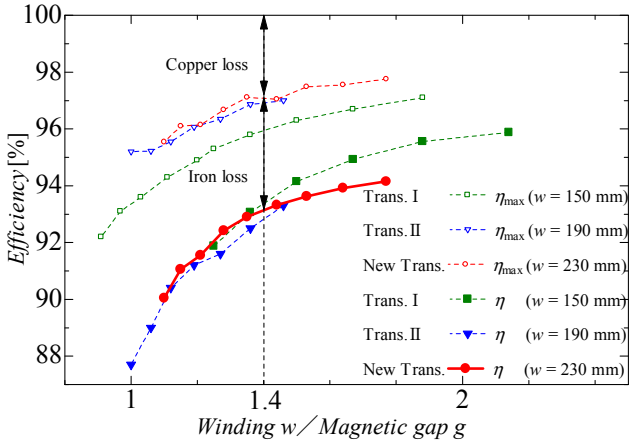

Figure 5. Relationship between η and w/g.

III. DESIGN OF A LARGE AIR GAP TRANSFORMER

A. *Decision on the Winding Width*

The coupling factor k decreases with an increase in the gap length. In the design of a large air gap transformer, it is necessary to increase the winding width to prevent a decrease in the coupling factor k. The coupling factor k depends on the ratio w/g, where w is the winding width, and g is the air gap length between the primary core and the secondary core. A larger value of w/g implies a larger value

(a) Picture

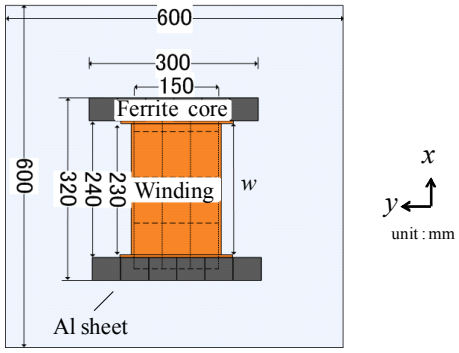

(b) Dimensions

Figure 6. Photograph and schematic of the 3 kW transformer.

TABLE II. SPECIFICATIONS OF THE 3 KW TRANSFORMER.

Type		H-shaped core
Litz wire		0.1 mmφ × 800
Weight of secondary transformer		5.5kg
Size		320 × 300 × 40 mm
Winding	*Primary*	20 T (3 parallel)
	Secondary	4 T (15 parallel)
Aluminum sheet		600 × 600 × 1 mm

of k. Fig. 5 shows the relationship among the maximum efficiency η_{max}, the experimental efficiency η, and w/g for three existing transformers. Here, the horizontal axis is w/g, and the vertical axis is the efficiency. The winding widths of the small gap transformers are 150 mm and 190 mm. Fig. 5 shows that a larger w/g ratio can achieve a higher efficiency. In addition, the η_{max} curves of the small gap transformers show the same characteristics, and the η curves also show the same characteristics. The difference in efficiency between η_{max} and η is considered an effect of the ferrite core loss. We designed the new large air gap transformer using the efficiency curves in Fig. 5.

In the design of a small air gap (70 mm) transformer, we set the target of the transformer efficiency η to be above 96%, and the w/g ratio is set to 2, as shown in Fig. 5. However, for a large air gap transformer, it is difficult to set

TABLE III. TRANSFORMER PARAMETERS.

f_0 [kHz]	50	
gap [mm]	160	200
k	0.18	0.12
R_{Lmax} [Ω]	12.8	15.7
η_{max} [%]	97.1	95.5
Q_1	345	329
Q_2	462	357

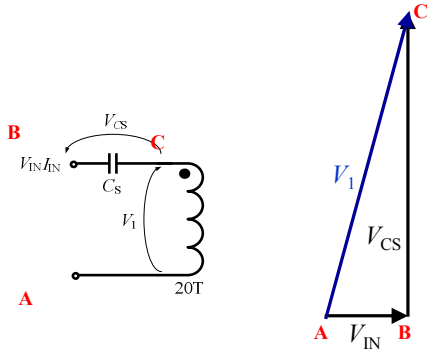

(a) Without split windings and capacitor

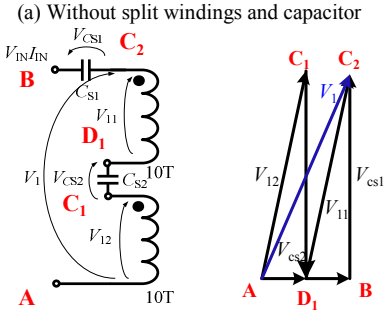

(b) With split windings and capacitors

Figure 7. Split winding voltage vector.

the w/g ratio to 2 because the secondary transformer must be compact in order to be installed in cars. We decided on a w/g ratio of 1.4 to get an efficiency above 92% at the normal air gap of 160 mm. Consequently, the winding width w is 230 mm.

B. Specifications of a Large Air Gap Transformer

Table II lists the specifications of a 3 kW double-sided winding transformer using an H-shaped core. Fig. 6 (a) shows a photograph of the transformer, and Fig. 6 (b) shows a schematic of the transformer with dimensions. Table III lists the transformer parameters for the normal position (mechanical gap length of 160 mm). The coupling factor k of the 160 mm air gap is approximately 0.18. The turn ratio is determined by (3) and is found to be 20 / 4 = 5, which is almost equal to the reciprocal of k [3]. Then, the output voltage V_2 is almost equal to the input voltage V_{IN}.

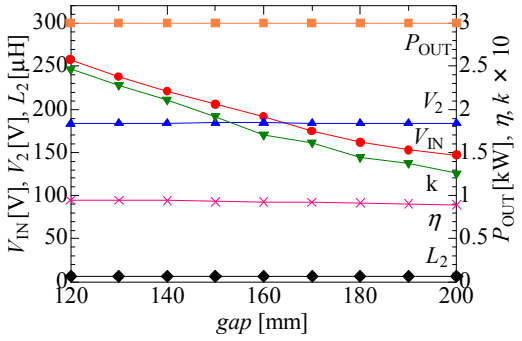

Figure 8. Transformer values with change in air gap.

TABLE IV. EXPERIMENTAL RESULTS.

P_{OUT} [W]	3000			
gap [mm]	160			200
x [mm]	0	100	0	0
y [mm]	0	0	200	0
V_{IN} [V]	217	168	162	167
V_1 [V]	501	621	676	643
V_2 [V]	213	213	213	213
V_L [V]	547	547	547	547
η [%]	92.9	90.1	88.9	90.0

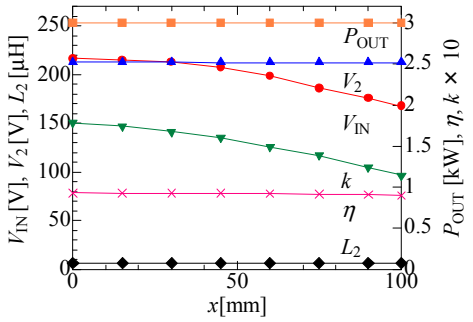

Figure 9. Transformer values with change in x position.

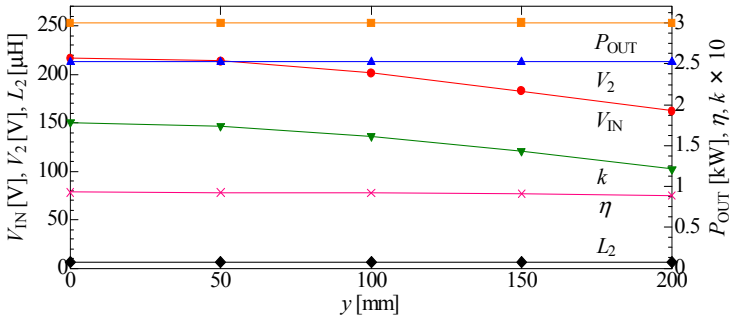

Figure 10. Transformer values with change in y position.

C. *Increasing of the Winding's Q Values*

As the winding's Q values are represented by (6), the easiest way to increase Q is to increase the frequency. Table III shows the winding's Q values for a 3 kW double-sided winding transformer using an H-shaped core at 30 kHz and 50 kHz. The winding's Q values at 50 kHz are about 20% higher than those at 30 kHz. To achieve a high efficiency, we chose to use 50 kHz.

D. *Avoidance of Primary Terminal Overvoltage*

The coupling factor k decreases with an increase in gap length, and the overvoltage of the primary terminal voltage V_1 (in Fig. 2) becomes a problem. The primary terminal voltage V_1 is represented by:

$$V_1 = \sqrt{V_{IN}^2 + (x_S I_{IN})^2} \tag{13}$$

In (13), $x_s I_{IN}$ becomes larger than V_{IN}, and the value of V_1 is mainly determined by $x_s I_{IN}$. The coupling factor k is equivalent to the value of b shown in (3). Thus, the primary current I_{IN} increases as the coupling factor k gets smaller. The primary terminal voltage V_1 increases with an increase in air gap length. The overvoltage of V_1 is not good for the series capacitor and the primary winding. To avoid high primary terminal voltage, the primary winding and the series capacitor are severally split into two, and the split windings and capacitors are alternately connected in series [7]. Fig. 7 (a) depicts the voltage vectors when the primary winding and the series capacitor are not split, and Fig. 7 (b) depicts those when they are split. Fig. 7 (b) shows the reduction in the capacitor voltage and the primary terminal overvoltage.

IV. EXPERIMENTAL RESULTS

When using wireless power transfer systems for EVs, misalignment due to the driver's skill and gap changes due to the car weight cannot be avoided. A mechanical gap length of 160 mm with no misalignment is taken to be the normal position. The transformer characteristics were measured for gap lengths in the range of 160 mm ± 40 mm, misalignments in the forward direction x of ± 100 mm, and misalignments in the lateral direction y of ± 200 mm. Misalignments in the x direction can be minimized using wheel stops, but a large misalignment tolerance in the y direction is required to allow for easy parking. Experiments were performed in the circuit shown in Fig. 2. The operating frequency f_0 was 50 kHz and was constant during the experiments. A double-voltage rectifier was used as a rectifier circuit on the second side to increase the efficiency. In the experiments, the capacitances of C_S and C_P remained constant during the experiments, and the load resistance R_L was kept constant at 100 Ω. A thick aluminum sheet (600 mm × 600 mm × 1 mm) was attached to the back of the transformer to shield the leakage flux.

A. *Characteristics with a Wide Gap*

Figs. 8 to 10 and Table IV show the transformer values when the gap length or position was changed. The mutual inductance M and the coupling factor k decreased with an increase in gap length or misalignment because the

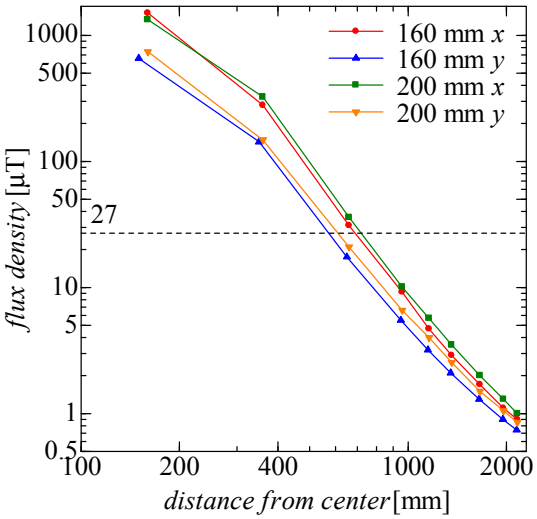

Figure 11. Leakages flux measurement (50 kHz).

magnetic reluctance of the main flux path became larger. However, the secondary self-inductance L_2 was almost constant; consequently, the capacitance of the parallel capacitor C_P given by (1) can be constant.

As shown in Figs. 8 to 10, the coupling factor k decreased when the gap length or the misalignment increased, and the ideal transformer turn ratio b decreased and the voltage ratio (V_2/V_{IN}) increased according to (3). The output power P_{OUT} remained constant at 3 kW when the input voltage V_{IN} was varied. The transformer experimental efficiency η at the normal position was 92.9% at 3 kW of output power, and the efficiency was 90% at a 200 mm air gap. From Fig. 5, the characteristics of the prototype transformer were similar to those of the conventional transformers.

B. *Characteristics with a Large Misalignment*

Figs. 9 and 10 show the transformer values when the position was changed. The efficiency η was 89% at maximum misalignment in the lateral y direction, and the output power was 3 kW. The 3 kW transformer was comparable to the conventional transformer in its positional deviation characteristics. Therefore, a large air gap 3 kW transformer was achieved.

C. *Characteristics of Leakage Flux*

Since the wireless power transformer has small coupling, the leakage flux is distributed around the transformer. In practical applications, the effects of leakage flux pose serious problems to human health. The leakage flux around humans must fall below the value specified by safety standards. Fig. 11 shows the criteria for exposure to electromagnetic lines; the 27 μT line represents the reference level for exposure to the general public given in ICNIRP2010 [8]. The coupling factor k decreased with an increase in gap length. Therefore, the influence of external electromagnetic flux leakage is a significant concern for large air gaps. Fig. 11 also shows the leakages flux densities of the 3 kW transformer at gap lengths of 160 mm and 200 mm. The electromagnetic flux leakages for the 160 mm and 200 mm air gaps were less than the reference levels for exposure to the general public given in ICNIRP2010 about 700 mm and 800 mm away from the center of the transformer, respectively. If the transformer is attached to the center of the car, it is safe for humans near the vehicle.

V. CONCLUSION

The maximum efficiencies of the inductive coupling methods and magnetic resonance methods are expressed by the same simple equations using the coupling factor k and the winding's Q if considering the copper loss only. The design procedure for the transformer of the inductive coupling type using this equation is proposed. The experimental results for the newly developed 3 kW transformer with an H-shaped core has a high efficiency (90%), a large air gap (200 mm), and good tolerance for misalignments in the lateral direction (± 200 mm) and is small in size (320 × 300 × 40 mm) and lightweight (5.5 kg).

ACKOWLEDGMENT

This research was sponsored by the New Energy and Industrial Technology Development Organization (NEDO) of Japan.

REFERENCES

[1] M. Budhia, G. A. Covic, and J. T. Boys, “A new magnetic coupler for inductive power transfer electric vehicle charging systems,” in proceedings of IEEE IECON 2010, pp. 2481–2486, 2010.

[2] M. Budhia, G. A. Covic, J. T. Boys and C. Y. Huang, “Development and evaluation of a single sided magnetic flux coupler for contactless electric vehicle charging,” in proceedings of IEEE ECCE 2011, pp. 614-621, 2011.

[3] M. Chigira, Y. Nagatsuka, Y. Kaneko, S. Abe, T. Yasuda and A. Suzuki, “Small-size light-weight transformer with new core structure for contactless electric vehicle power transfer system,” in proceedings of IEEE ECCE 2011, pp. 260–266, 2011.

[4] A. Kurs, A. Karalis, R. Moffatt, J. D. Joannopoulos, P. Fisher and M. Soljačić, “Wireless power transfer via strongly coupled magnetic resonances,” Science Express, vol. 317, no. 5834, pp. 83–86, 2007.

[5] T. Imura, T. Uchida and Y. Hori, “Basic experimental study on helical antennas of wireless power transfer for electric vehicles by using magnetic resonant couplings,” in proceedings of IEEE Vehicle Power and Propulsion Conference, pp. 936-940, 2009.

[6] T. Tohi, Y. Kaneko and S. Abe, “Maximum efficiency of wireless power transfer systems using k and Q,” IEEJ Transactions on Industry Applications, vol. 132, no.1, pp. 123–124, 2011 (in Japanese).

[7] T. Yamanaka, Y. Kaneko, S. Abe and T. Yasuda, “10 kW Contactless Power Transfer System for Rapid Charger of Electric Vehicle,” in proceedings of the 26th International Battery, Hybrid and Fuel Cell Electric Vehicle Symposium, EVS26, Los Angeles, California, pp.1-9, 2012.

[8] International Commission on Non-Ionizing Radiation Protection (ICNIRP), “Guidelines for limiting exposure to time varying electric, magnetic, and electromagnetic fields,” 2010.